

## Supplementary Information

### Hydrogen transport property of polymer-derived cobalt cation-doped amorphous silica

Shotaro Tada<sup>1</sup>, Shiori Ando<sup>1</sup>, Toru Asaka<sup>1</sup>, Yusuke Daiko<sup>1</sup>, Sawao Honda<sup>1</sup>, Samuel Bernard<sup>2</sup> & Yuji Iwamoto<sup>\*1</sup>

<sup>1</sup>Department of Life Science and Applied Chemistry, Graduate School of Engineering, Nagoya Institute of Technology, Gokiso-cho, Showa-ku, Nagoya 466-8555, Japan

<sup>2</sup>University of Limoges, CNRS, IRCER, UMR 7315, F-87000, Limoges, France

\* Corresponding author: Yuji Iwamoto

E-mail: [iwamoto.yuji@nitech.ac.jp](mailto:iwamoto.yuji@nitech.ac.jp)

Tel/Fax: +81-52-735-5276

### Keywords.

Co-doped amorphous silica

Polymer-derived ceramics (PDCs),

Hydrogen transport

Hydrogen-bonded Si-OH

Divalent Co cation (Co<sup>2+</sup>)

Hydrogen /deuterium isotope exchange (OH/OD conversion)

To study the reactivity toward H<sub>2</sub>, hydrogen (H) / deuterium (D) isotope exchange in the silanol groups (Si-OH/OD conversion) of the polymer-derived Co-doped amorphous silica was in-situ monitored by measuring IR absorption spectroscopy adopted diffuse reflectance infra-red Fourier transform spectroscopy (DRIFTS) technique (Model Spectrum 100, Perkin Elmer, Waltham, MA, USA). according to the following procedure:

The 600 °C-heat treated sample was placed within a diffuse reflection cell (Model STJ900C Diffuse IR Heat Cham, S.T. JAPAN Inc., Tokyo, Japan), and subjected to pre-drying to remove adsorbed water at 500 °C for 20 h under an argon (Ar) flow (4 ml/min). The sample was subsequently heat-treated at 500 °C for an additional 3 h under a hydrogen flow (4 ml/min), and the initial IR spectrum was recorded. Then, under a flowing 10% deuterium (D<sub>2</sub>) /Ar (4 ml/min) at 500 °C, the Si-OH/OD conversion was in-situ monitored by measuring DRIFT spectra at a specific time interval of 1, 5, 10, 20, 30, 60, 90, 12, 150 and 180 min.

The DRIFT spectra for non-doped and Co-doped amorphous silica (Co/Si atomic ratio of 0.18, 0.05, 0.03 and 0.01) before and after Si-OH/OD conversion (at 180min) were shown in Fig.SI1. In addition to the sharp adsorption band assigned to free Si-OH at around 3730 cm<sup>-1</sup>, the spectrum exhibited a broad absorption band at around 3685 cm<sup>-1</sup> attributed to hydrogen (H)-bonded Si-OH groups for all the Co-doped amorphous silica samples. The OH/OD conversion for the free Si-OH and the H-bonded Si-OH was successfully monitored for all the Co-doped samples.

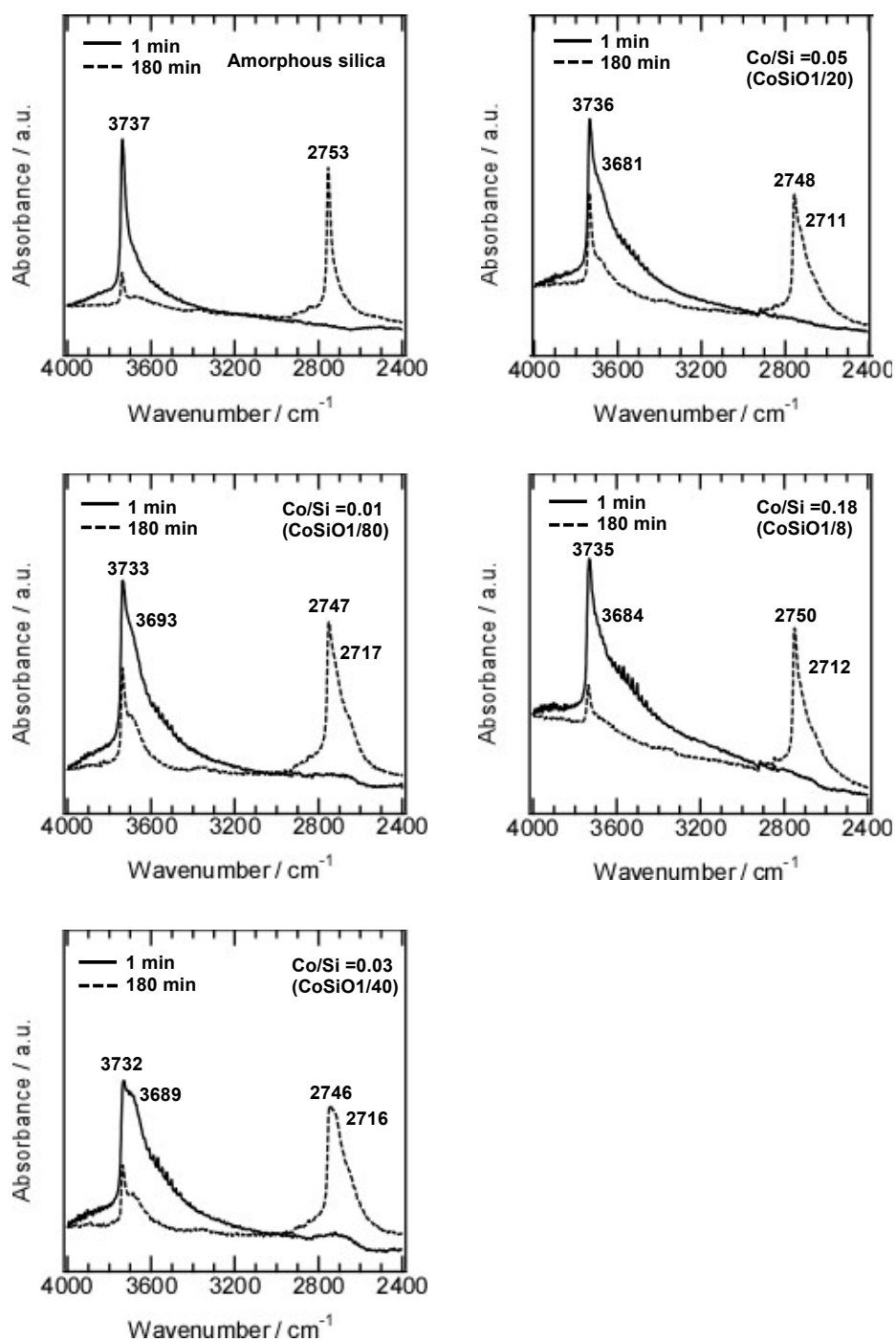


**Fig. S11.** Si-OH/OD conversion of amorphous silica and Co-doped amorphous silica in-situ monitored by measuring DRIFT spectra under 10%D<sub>2</sub>/Ar flow at 500 °C.

In the present study, the hydrogen self-diffusion coefficient ( $D$ ) at the surface was adopted as an index of Si-OH/OD conversion rate on the non-doped and Co-doped amorphous silica surface. The parameters of  $D$  and  $c_{D\text{ eq}}$  (the equilibrium deuterium concentration of the sample) were evaluated by employing Eq. (3). Fig. SI.2 presents the  $D_2$  exposure time dependence of the absorption band intensity evaluated for the free Si-OD and the D-bonded Si-OD for all samples. Each fitted line described the experimental data very well, which suggesting OH/OD conversions for both the free and H-bonded Si-OH investigated in this study were diffusion controlled.

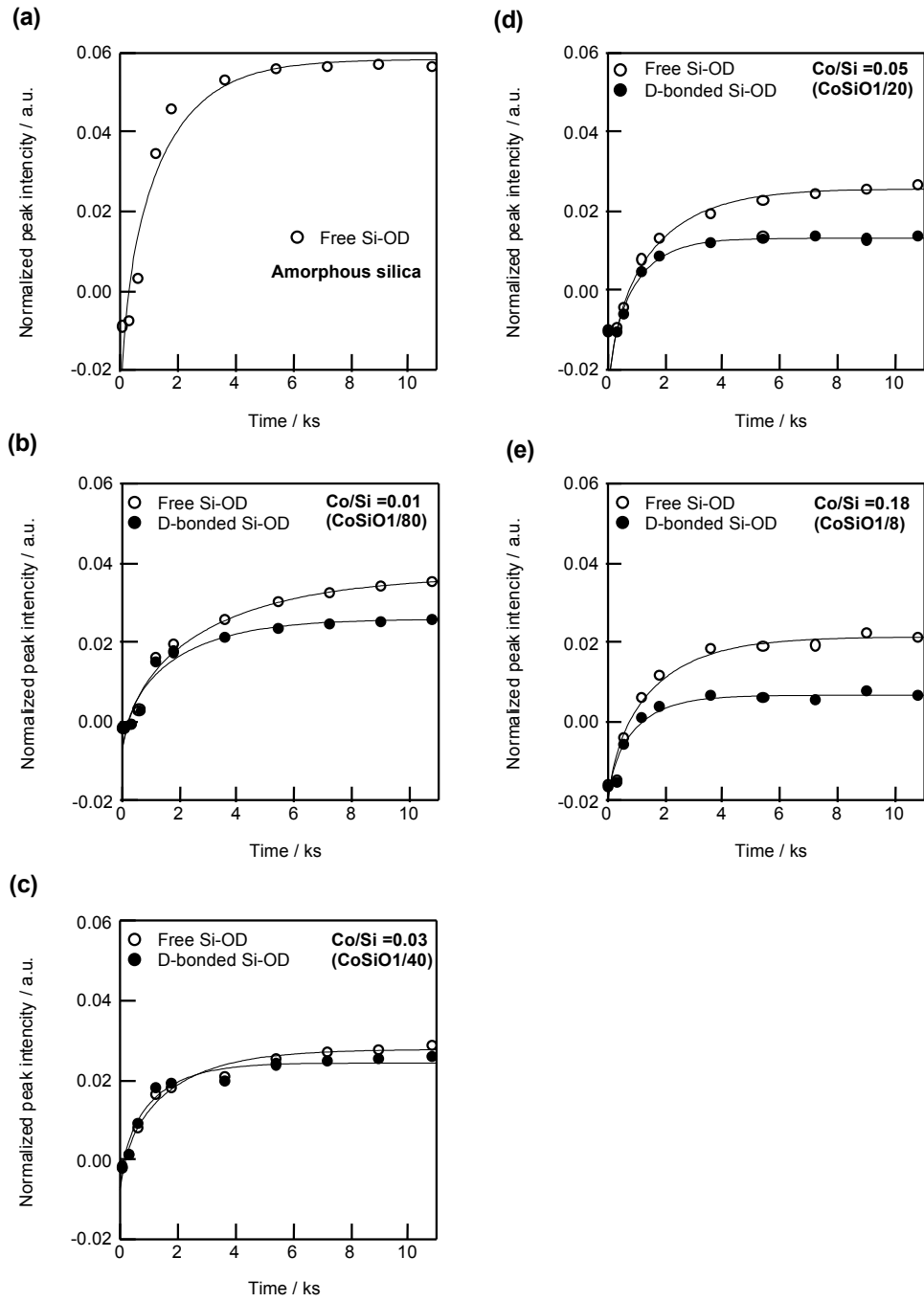


**Fig. S12.** OH/OD conversion for surface silanol groups of non-doped and Co-doped amorphous silica.

Transmission electron microscope (TEM) observations and high-angle annular dark-field-scanning transmission electron microscope (HAADF-STEM) observations were performed on the 600 °C heat-treated powder samples (SiCo201 and SiCo81) in a JEOL JEM-ARM200F operated at an accelerating voltage of 200 kV. The size of the electron probe was approximately 0.1 nm. The convergent angle and the detector collection angle were 22 mrad and 68-280 mrad, respectively. Analytical investigations were carried out by electron energy loss spectroscopy (EELS) using a Gatan Quantum ERS with an incident-electron beam-energy of 200 keV.

The size distribution of Co-species within the amorphous silica-based matrix characterized for the Co-doped amorphous silica with the analytical Co/Si atomic ratio of (a) 0.05 (SiCo201) and (b) 0.18 (SiCo81) was shown in Fig. SI3. As shown in Fig. SI3(a), the SiCo201 exhibited a narrow and unimodal spot size distribution, and the mean size was determined as 1.8 nm. On the other hand, the SiCo81 showed a wider size distribution with a larger mean size of 3.4 nm (Fig. SI3(b)).

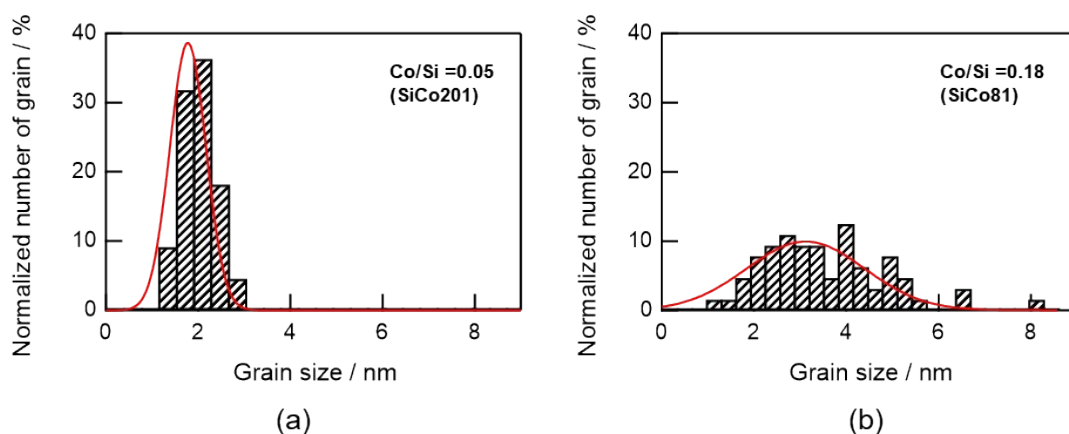


**Fig. SI3.** The size distribution of Co-species within the amorphous silica-based matrix characterized for the Co-doped amorphous silica with the analytical Co/Si atomic ratio of (a) 0.05 (SiCo201 sample) and (b) 0.18 (SiCo81 sample).

Then to study on the Co-cluster formation in more details, STEM observation was performed on the samples with  $\text{Co/Si} = 0.01$  (**CoSiO1/80** sample) and  $\text{Co/Si} = 0.03$  (**CoSiO1/40** sample). These samples with lower Co/Si ratio below 0.05 exhibited feature less nanostructures. Then, intensive STEM observation was performed. As a result, **CoSiO1/80** sample exhibited a trace amounts of bright spots with a size of about 1-2 nm under the ADF-STEM imaging mode (Fig. SI4). It was also rare for the **CoSiO1/40** sample. However, we found some spots suggested as Co cluster with less than 2 nm in size (Fig. SI5).

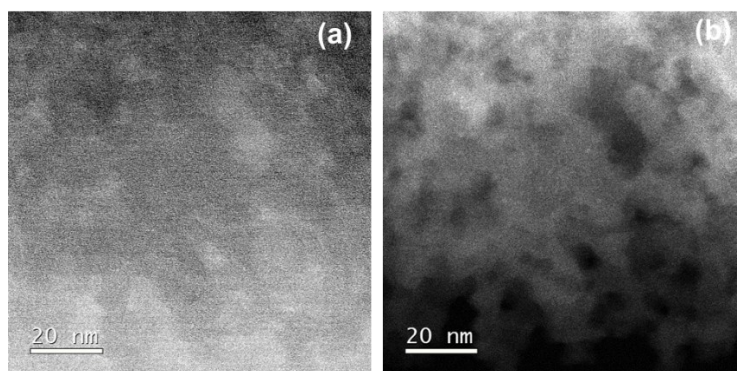


**Fig. SI4.** Nanostructure observation of Co-doped amorphous silica with  $\text{Co/Si} = 0.01$  (**CoSiO1/80** sample). (a) BF-STEM image and (b) ADF-STEM image.

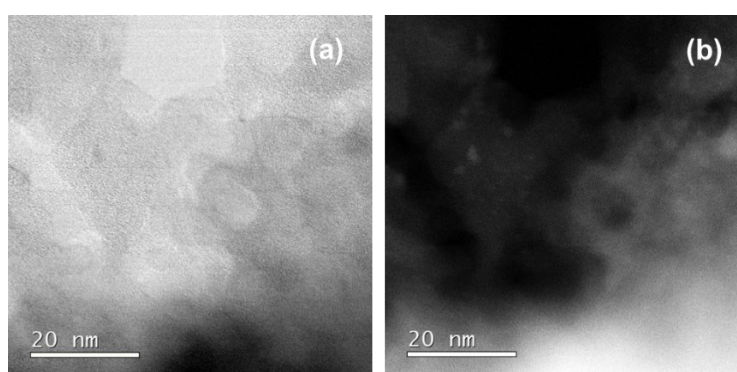


**Fig. SI5.** Nanostructure observation of Co-doped amorphous silica with  $\text{Co/Si} = 0.03$  (**CoSiO1/40** sample). (a) BF-STEM image and (b) ADF-STEM image.

The relation between the  $c_{D\text{eq}}$  and  $D$  (H-bonded) was further examined by additional plot of the  $c_{D\text{eq}}$  dependence of  $\nu(\text{OH})$  of the H-bonded Si-OH detected by FTIR spectroscopic analysis. As shown in Fig. SI6, the  $\nu(\text{OH})$  slightly shifted toward lower wavenumber consistently with the  $c_{D\text{eq}}$  as well as  $D$  (H-bonded). Accordingly, the acidity of the H-bonded Si-OH increased with the  $c_{D\text{eq}}$ , *i.e.* the number of the Co(II)-induced H-bonded Si-OH with in the amorphous silica matrix. Thus, in addition to the increase in the number of the  $\text{Co}^{2+}$ -induced H-bonded Si-OH, the acidity of the H-bonded Si-OH increased with the  $c_{D\text{eq}}$ , which resulted in the increase in the  $D$  (H-bonded) consistently with  $c_{D\text{eq}}$ .

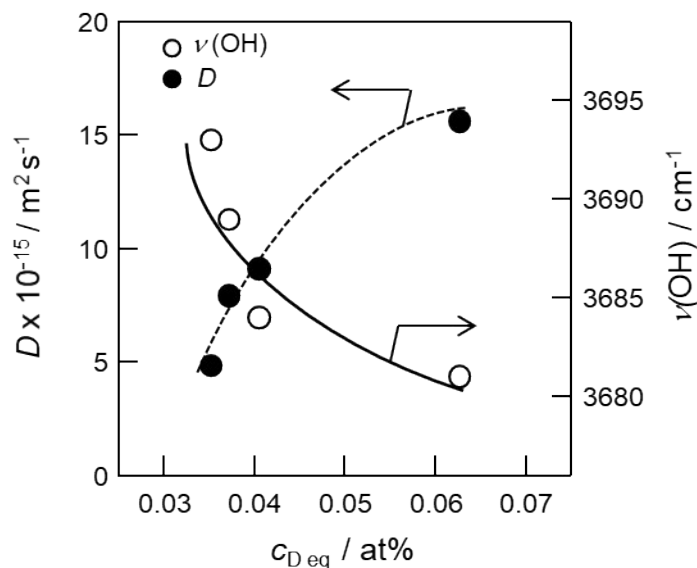


**Fig. SI6.**  $c_{D\text{eq}}$  dependence of  $\nu(\text{OH})$  of the H-bonded Si-OH detected by FTIR spectroscopic analysis in comparison with that of  $D$  (H-bonded).